Research Square

Preprints are preliminary reports that have not undergone peer review.
They should not be considered conclusive, used to inform clinical practice,
or referenced by the media as validated information.

Liquefaction assessment using alternative approaches: a case study of Ho Chi Minh City stratigraphy

NHAT-PHI DOAN

doannhatphi@iuh.edu.vn

Industrial University of Ho Chi Minh City https://orcid.org/0000-0003-3953-5443

Van Nam Nguyen

Industrial University of Ho Chi Minh City

Duy Triet Doan

Vinh Long University of Technology Education

Sung-Sik Park

Kyungpook National University

Research Article

Keywords: liquefaction, factor of safety to liquefaction, settlement, liquefaction potential index, liquefaction severity number

Posted Date: March 14th, 2023

DOI: https://doi.org/10.21203/rs.3.rs-2667778/v1

License: This work is licensed under a Creative Commons Attribution 4.0 International License.
Read Full License

Additional Declarations:
Competing interests: The authors declare no competing interests.

Version of Record: A version of this preprint was published at Geosciences Journal on March 27th, 2024.
See the published version at https://doi.org/10.1007/s12303-024-0006-4.

Liquefaction Assessment Using Alternative Approaches: A case study of Ho Chi Minh City Stratigraphy

Nhat-Phi Doan[1*], Van Nam Nguyen[1], and Duy Triet Doan[2], and Sung-Sik Park[3]

1 Department of Civil Engineering, Industrial University of Ho Chi Minh City, 12 Nguyen Van Bao, Ward 4, Go Vap District, Ho Chi Minh City 700000, Vietnam

2 Department of Mechanical Dynamics, Vinh Long University of Technology Education, Vinh Long 890000, Vietnam

3 Department of Civil Engineering, Kyungpook National University, 1370 Sankyuk-dong, Buk-gu, Daegu 702-701, Korea

Nhat-Phi Doan: doannhatphi@iuh.edu.vn, Lecturer

Van Nam Nguyen: nguyenvannam@iuh.edu.vn, Lecturer

Duy Triet Doan: trietdd@vlute.edu.vn, Lecturer

Sung-Sik Park: sungpark@knu.ac.kr, Professor

*Corresponding author: Nhat-Phi Doan

Department of Civil Engineering, Industrial University of Ho Chi Minh City, 12 Nguyen Van Bao, Ward 4, Go Vap District, Ho Chi Minh City 700000, Vietnam

Phone: +84 (0) 939 113 170

Email: doannhatphi@iuh.edu.vn ORCID: https://orcid.org/0000-0003-3953-5443

Running title: Liquefaction Assessment Using Alternative Approaches: Ho Chi Minh Strata

Abstract: Liquefaction has been known as a phenomenon in which the shear strength and stiffness of saturated soil are reduced by the generation of pore water pressure under earthquake loading. Consequently, liquefaction-induced settlement can result in severe damages including building cracks or slope failure, which pose a threat to human lives and properties. In the current Vietnamese standard TCVN 9386:2012, liquefaction potential hazard is often evaluated using the simplified method, which solely identifies the areas with a high risk of liquefaction. Prediction of Safety Factor (FS), Settlement (S), Liquefaction Potential Index (*LPI*), and Liquefaction Severity Number (*LSN*) has not received sufficient attention to a completeness standard. This study assesses the liquefaction of the ground at Ho Chi Minh City, Vietnam by using four conventional methods: the simplified procedure, linear equivalent analysis, loosely-coupled effective stress analysis, and fully-coupled effective stress analysis based on standard penetration test (SPT) data in Ho Chi Minh Metropolitan City. A class of seismic events that are compatible with the design response spectrum in the Vietnamese standard TCVN 9386:2012 is used as input ground motion at the bedrock. According to the results of different methods, maps of ground settlement, *LPI,* and *LSN* are proposed as useful references for construction works on such ground, which may have a high potential for liquefaction and subsidence.

Keywords: liquefaction, factor of safety to liquefaction, settlement, liquefaction potential index, liquefaction severity number.

1. INTRODUCTION

Earthquake-induced liquefaction has been considered one of the primary hazards that lead to severe damage to soil-structures built on saturated deposits (Le et al., 2022a, 2022b; Nguyen et al., 2018, 2017; Rahman et al., 2021). Liquefaction from recent earthquakes such as the 1994 Northridge, 1999 Kocaeli, 1999 Chi-Chi, 2005 Kashmir, 2008 Wenchuan, 2010 Chile, 2010 and 2011 Newzealand, Tohoku 2011, was observed to result in many large deformations (i.e., settlement and horizontal displacements) leading to catastrophic damages to soil-structures built on the liquefied ground.

To evaluate a seismic site response from a design earthquake event, three stages are often pronounced involving the estimation of (i) cyclic stress ratio (*CSR*), (ii) cyclic resistance ratio (*CRR*), and (iii) factor of safety (*FS*) to identify zones that will liquefy. Then, a further assessment of the liquefaction potential index (*LPI*), liquefaction severity of number (*LSN*), and ground settlement can be carried out based on the results of the FS. To estimate the *CSR*, the simplest way is using the total stress-based analysis, which is often performed to identify regions with a high potential of liquefaction. In this approach, displacement is calculated by reducing the strength material to its residual strength and the pore water pressure generation is omitted. Therefore, there is an argument about the resulting displacements obtained from this method due to its oversimplifications (Galavi et al., 2013). The advanced analysis is the effective stress-based analysis, in which the element response is a function of evolving effective stress state (Beaty and Perlea, 2011). Herein, the pore pressure changes and volumetric strain related to ground settlement are predicted in the formulation.

Since the 1970s, a methodology termed the ‘simplified procedure’ has evolved as a standard of practice for evaluating the liquefaction resistance of soils. Following disastrous

earthquakes in Alaska and Niigata, Japan in 1964, Seed and Idriss (1971) developed and published the basic 'simplified procedure'. That procedure has been modified and improved periodically since that time (Youd et al., 2001). For example, the simplified method based on SPT data Youd et al. (2001), Cetin et al. (2004), Boulanger and Idriss (2014); CPT data – Youd et al. (2001), Moss et al. Moss et al. (2006), Idriss and Boulanger (2008); $V_{s\,\mathrm{data}}$ – Andrus and Stokoe (2000), Kayen et al. (2013).

An equivalent linear procedure is used to predict the transformation of seismic motions as they generate upward through a soil profile (Idriss and Seed, 1968; Seed and Idriss, 1970). From the equivalent uniform strain induced in each sublayer, values of modulus and damping can be predicted throughout an iterative procedure. Based on this, Schnabel (1972) firstly proposed the 1D equivalent linear site response analysis, which is well-known as the original SHAKE program. After two decades of development with many updates, SHAKE91 (Idriss and Sun, 1992) has been known as the standard equivalent linear code. To date, numerous following codes have been developed in advance based on it.

The loosely coupled (i.e., partial coupled) effective stress-based analysis, in which the element response is a function of evolving effective stress state (Beaty and Perlea, 2011). Herein, the pore pressure changes are predicted by an independent pore pressure generator and do not relate to the volumetric strains produced by the soil skeletons. These models may be the extensions of perfect plastic models or complex non-linear models, for example, the Finn-Byrne model (Byrne, 1991; Finn, 1985) implemented in FLAC software (Itasca Consulting Group Inc., 2011).

Fully coupled effective stress-based models are the most sophisticated continuum models for the assessment of liquefaction. The dilative or contractive behavior of sand can be directly predicted with each load cycle. The changes in pore water pressure can be estimated in response

93 to the contraction or dilation of the soil skeleton. However, the calibration and verification of these
94 models are often complex since the pore pressure response and stiffness depend on the appropriate
95 prediction of volumetric strains at each lading cycle. With the advancement of computer
96 technology in the twentieth century, several fully coupled constitutive models have been developed
97 to predict the liquefaction phenomenon. Many robust models such as UBCSAND (Beaty and
98 Byrne, 2011; S. S. Park et al., 2021) and PM4SAND (Boulanger and Ziotopoulou, 2015) have
99 been proposed or developed and implemented in commercial programs (FLAC, PLAXIS) for
100 applications in practical earthquake engineering analyses.

101 From 113 to 2003, a total of 1645 earthquake events have been recorded in Vietnam with
102 a magnitude (M_L) of 3.0 or higher (Ngo et al., 2008; Nguyen and Nguyen, 2022; Nguyen et al.,
103 2020; Tran et al., 2021). Among that, up to 90% of the events were found in Northern Vietnam
104 (Hung, 2012; Nguyen and Nguyen, 2022), since the Indochina and South China faults are operating
105 in the area. Southern Vietnam was always expected as a region with low tectonic activities,
106 compared to the North. However, recent earthquakes with a moderate magnitude that appeared
107 offshore of Vung Tau city in August 2005 (M_L = 4.5), or Binh Thuan province in 2020 (M_L = 4.7)
108 related to the Thuan Hai – Minh Hai fault (Nguyen and Nguyen, 2022), have threatened the densely
109 populated areas such as Ho Chi Minh city (185 km from the epicenter). It is not excessive if site
110 response analysis of Ho Chi Minh stratigraphy would be carried out to mitigate damages and losses
111 from large earthquake-induced liquefaction. Currently, Vietnamese standard TCVN 9386:2012
112 (Vietnam National Code, 2012) has been used to evaluate the potential liquefaction, in which the
113 basis of the simplified method is solely applicable. However, a boundary of the application is
114 somehow to initially identify liquefied zones. Numerous papers with regard to the potential
115 liquefaction analysis of Northern Vietnam have been published (Chi and others, 2017; Nhung et

al., 2018, 2017; Nu et al., 2021). It is noted that maps of *LPI* in Hanoi city were presented by Nhung et al. (2017) and estimations of *FS*, *LPI*, and *LSN* were performed in the findings of Nu et al. (2021), Nhung et al. (2017, 2018). Hua et al. (2017) reported the results of *FS* and designed earthquake-induced volumetric strains based on stratigraphy of the coastal seashore in Middle Vietnam. Pham and Dai Vo (2014) partially showed an *LPI* map of District 7 – Ho Chi Minh City, however, it is inapplicable to the whole city. Generally, the simplified method has been widely used in the aforementioned research. Interestingly, the equivalent linear analysis (i.e., SHAKE computer codes) and non-linear site response analysis (i.e., DEEP-SOIL computer codes) have been recently applied to 1D site response analyses for Ha Noi city (Nguyen et al., 2020; Tran et al., 2021) and Can Tho city (Nguyen and Nguyen, 2022). However, their research has just focused on the analyses of the response spectrum, shear strains, and peak ground acceleration (*PGA*) between observed layers and total stress-based analysis has been still employed. There has been still an absence from the literature review of a general scheme such as maps of *LPI*, *LSN*, and ground settlement for a specific stratigraphy in Vietnam considered alternative approaches.

In this paper, the total stress-based analysis is used for simplified method and equivalent linear analysis, meanwhile, the effective stress analysis in terms of loosely-coupled and fully-coupled effective stress models are employed for one-dimensional (1D) ground response analysis. A series of SPT data from different districts around Ho Chi Minh city was considered as input soil parameters for (i) simplified method using Boulanger and Idriss (2014)'s liquefaction triggering empirical relationships; (ii) equivalent linear analysis using SHAKE91 computer code; (iii) loosely-coupled effective stress analysis using Finn-Byrne model; and (iv) fully-coupled effective stress analysis using UBCSAND model, respectively. Analytical and numerical results from the four methods are taken into account for a completeness comparison concerning the evaluations of

139 *CSR*, *FS*, maximum shear strain (γ_{max}), maximum volumetric strain (ε_v), ground settlement (*S*),
140 *LPI*, *LSN*, and excess pore water pressure ratio (R_u). Based on that, an objective point of view is
141 provided to see the merits and drawbacks of each method.
142
143 **2. PROCEDURE FOR EVALUATION OF SOIL LIQUEFACTION**
144 **2.1. Cyclic stress ratio (CSR)**
145
146 The cyclic stress ratio *CSR* is the ratio of cyclic shear stress τ_{cyc} to the vertical effective
147 stress σ'_{v0} during the seismic loading. *CSR* can be calculated as follows:
148 $$CSR = \frac{\tau_{xy}}{\sigma'_{v0}} \quad (1)$$
149 The *CSR* is widely used in the "simplified procedure" introduced by Seed and Idriss (1971) to
150 evaluate the potential of liquefaction, which can be calculated by the maximum acceleration of
151 earthquake motion a_{max}, overburden stress σ'_{v0} and flexibility of soil profile.
152
153 **2.1.1. Simplified method**
154 In this method, *CSR* can be expressed as follows:
155 $$CSR = \frac{\tau_{av}}{\sigma'_{v0}} = 0.65\left(\frac{\sigma_{v0}}{\sigma'_{v0}}\right)\left(\frac{a_{max}}{g}\right)r_d \quad (2)$$
156 $$r_d = \exp\left[\alpha(z) + \beta(z).M\right] \quad (3)$$
157 $$\alpha(z) = -1.012 - 1.126 \times sin\left(\frac{z}{11.73} + 5.133\right) \quad (4)$$
158 $$\beta(z) = 0.106 + 0.118 \times sin\left(\frac{z}{11.28} + 5.142\right) \quad (5)$$
159
160 where a_{max} = maximum acceleration at ground surface induced by earthquake. g = gravity
161 acceleration, σ'_{v0} and σ_{v0} are the effective and total vertical overburden stress. r_d = stress reduction

factor considering the flexibility of soil profile, and the version used in this paper is from Idriss (1999) and Golesorkhi (1989). z = depth below ground surface in meters. The constant 0.65 is used to convert irregular earthquake loading into equivalent uniform cyclic loading.

2.1.2. Equivalent linear analysis

The equivalent-linear method estimates the nonlinear relationship between stress and strain for each layer in a soil profile by utilizing shear modulus reduction and damping curves. An iterative process is employed to calculate the degraded soil properties due to strain-induced nonlinearities. For the first stage of the algorithm, the behavior of the soil profile is estimated by utilizing small-strain values of shear modulus and damping. A shear strain timeline response is determined using the preliminary shear modulus and damping values, with the soil properties staying constant from the initiation to the end of the seismic motion. Based on this time history response for each layer, a representative shear strain, γ_{eff}, is selected. The chosen representative strain is utilized to determine the degraded values of shear modulus and damping, and these will be used in the subsequent iteration of the analysis. This sequence is repeated until the modulus and damping values attain a reasonable convergence with the predetermined degradation curves. Over time, various approaches and values have been employed to calculate the effective shear strain, γ_{eff}. Today, the most widely accepted approach is to utilize an effective strain value of 65% of the maximum shear strain.

In this paper, the SHAKE91 code was used to account for the equivalent linear site response analysis. A typical soil profile obtained from the SPT data at Ho Chi Minh Metropolitan City was performed in the analysis and a class of seismic events compatible with the design response spectrum in the Vietnamese standard TCVN 9386:2012 are used as input ground motion at the bedrock.

2.1.3. Loosely-couple effective stress analysis

In the effective stress-based analyses, the changes in effective stress due to cyclic loading are coupled in the formulation. While the pore pressure changes are estimated by an independent pore pressure generator, which is inconsistent with the volumetric strain produced by the model, they can be classified as the loosely-coupled (i.e., partially coupled) effective stress analyses. The loosely-coupled effective stress model used in this study was the Finn-Byrne model, which is available as a built-in model in the commercial software FLAC2D (Itasca Consulting Group Inc., 2011). This model incorporates two relationships between the irrecoverable volume-strain and the cyclic shear-strain amplitude, developed by (i) Martin et al. (1975) and (ii) Byrne (1991), into the Mohr-Coulomb model to estimate the dynamic pore pressure generation from shear stress cycles. In practice applications, the Finn model adopting Byrne (1991)'s relationship, known as the Finn-Byrne model, has been predominantly employed due to its simplicity and convenience. A detailed implementation and parametric study of this model can be found in Itasca (Itasca Consulting Group Inc., 2011). The general parameters of the Finn-Byrne model in this study are depicted in Table 1.

2.1.4. Fully-coupled effective stress analysis

The effective stress model used in this study was the UBCSAND model. This model was implemented by a user-defined subroutine under two-dimensional (2D) plane strain: the explicit finite difference program FLAC2D version 7.0 (Itasca Consulting Group Inc., 2011). It was developed for application to cyclic loads such as earthquakes based on the fully elastic-plastic Mohr-Coulomb model. The key input parameter of this model is the corrected SPT data $(N_1)_{60}$ of the site's ground. Many researchers have applied the UBCSAND model to laboratory tests and

practical seismic designs (Doan, 2021; Doan et al., 2020a, 2020b; B.-P. Nguyen et al., 2022; Nguyen et al., 2021b, 2021a; T. Nguyen et al., 2022; S.-S. Park et al., 2021; S. S. Park et al., 2020; S.-S. Park et al., 2020). A detailed explanation and verification of this model were described by Puebla et al. (1997), Byrne et al. (2004) and Beaty and Byrne (2011). The general parameters of the UBCSAND model in this study are depicted in Table 2.

2.2. Cyclic resistance ratio (CRR)

Generally, cyclic resistance to liquefaction is defined as the *CSR* at which a soil sample will reach liquefaction after the application of 15 cycles. This paper used the SPT-based method of Boulanger and Idriss (Boulanger and Idriss, 2014) to evaluate the *CRR*. The procedure is presented in Equation (6).

$$CRR_{7.5} = exp^{\left\{\frac{(N_1)_{60}}{14.1}+\left(\frac{(N_1)_{60}}{126}\right)^2-\left(\frac{(N_1)_{60}}{23.6}\right)^3+\left(\frac{(N_1)_{60}}{25.4}\right)^4-2.8\right\}} \quad (6)$$

where $(N_1)_{60}$ is the corrected SPT number of blow counts.

2.3. Magnitude scaling factor (MSF)

Since the $CRR_{7.5}$ are related to an earthquake magnitude of 7.5, the *MSF* is introduced to adjust the value to the target event magnitude. The conversion relationship of Boulanger and Idriss (2014) has been used in this paper, which can be expressed in Equation (7).

$$MSF = 1 + (MSF_{max} - 1)\left\{8.64 \times e^{-(M/4)} - 1.325\right\} \quad (7)$$

$$MSF_{max} = 1.09 + \left(\frac{(N_1)_{60}}{31.5}\right)^2 < 2.2 \quad (8)$$

$$CRR = CRR_{7.5} \times MSF \quad (9)$$

where $(N_1)_{60}$ is the corrected SPT number of blow counts. Then, the *CRR* with regard to the target earthquake magnitude can be obtained from Equation (9).

2.4. Factor of safety (FS)

The key output to evaluate the soil likely to be liquefied is the safety factor, which can be defined as a ratio of *CRR* to *CSR*:

$$FS = CRR/CSR \times K_\sigma \times K_\alpha \quad (10)$$

where K_α = ground slope correction (is considered 1.0 in this study because of level ground analysis). K_σ = overburden stress correction factor, which can be expressed as in Equation (11).

$$K_\sigma = \left(\sigma'_{v0}/P_a\right)^{f-1} \quad (11)$$

where P_a is atmospheric pressure in the chosen units and f depends on relative (D_R) and is given by:

$$f = 1 - 0.005D_R \text{ for } 40\% < D_R < 80\% \quad (12)$$

$$D_R = (N_1)_{60}/46 \quad (13)$$

Based on the results of *FS*, other important outputs for liquefaction assessment such as *LPI* and *LSN* can be easily estimated.

2.5. Liquefaction potential index (LPI)

Calculation of the *LPI* is used to interpret the liquefaction assessment calculations in terms of severity over depth. The calculation procedure is based on the methodology developed by Iwasaki et al. (1984).

To estimate the severity of liquefaction extent at a given site, *LPI* is calculated based on the following equation:

$$LPI = \int_0^{20} (10 - 0.5z) \times F_L \times dz \quad (14)$$

where:

$F_L = 1 - FS$ when $FS < 1$

$F_L = 0$ when $FS > 1$

z is the depth of measurement in meters

Values of *LPI* range between zero (0) when no test point is characterized as liquefiable and 100 when all points are characterized as susceptible to liquefaction. Iwasaki et al. (1984) proposed four (4) discrete categories based on the numeric value of *LPI*:

$LPI = 0$: Liquefaction risk is very low

$0 < LPI <= 5$: Liquefaction risk is low

$5 < LPI <= 15$: Liquefaction risk is high

$LPI > 15$: Liquefaction risk is very high

2.6. Liquefaction severity number (LSN)

The *LSN* is a newly calculated parameter developed by Tonkin & Taylor consultant company (van Ballegooy et al., 2014) to reflect the more damaging effects of shallow liquefaction on residential land and foundations. The equation used to calculate *LSN* is presented below. *LSN* considers depth-weighted calculated volumetric densification strain within soil layers as a proxy for the severity of liquefaction land damage likely at the ground surface. The published strain calculation techniques consider strains that occur where materials have a calculated triggering *FS*

that reduces below 2.0. This means that the *LSN* begins to increase smoothly as factors of safety drop, rather than when the *FS* reaches 1.0. One other aspect of *LSN* to note is that strains self-limit based on the initial relative density as the factor of safety drops, so a given soil profile has a maximum *LSN* that it tends towards as the *PGA* increases.

$$LSN = 1000. \int \frac{\varepsilon_v}{z} dz \quad (15)$$

where ε_v is the calculated volumetric densification strain in the subject layer from Zhang et al. (2002). z is the depth to the layer of interest in meters below the ground surface.

The procedure for the estimation of seismic-induced settlements based on Robertson and Shao (2010). This procedure can be only used for the simplified method since the volumetric strain and settlement can be directly obtained from the effective stress analysis. Unfortunately, the volumetric strain or settlement cannot be estimated in the equivalent linear analysis although the reduction of shear modulus and damping ratio of soil are considered. As a result, there is an absence of the prediction of *LSN* and volumetric or settlement of the equivalent linear analysis in the results.

3. GEOTECHNICAL DATA

A collection of SPT data from 24 districts (i.e., one borehole for each district) in Ho Chi Minh City has been selected for analysis. Based on the available database, the information and location of selected SPT boreholes are summarized in Table 3 and Figure 1. It is noted that the target *PGA* is accordingly included in relevant to the TCVN 9386:2012 (Vietnam National Code, 2012), in which the representative shaking intensity level for an earthquake return period of 475 years is expected to Ho Chi Minh soil stratigraphy. Furthermore, the TCVN 9386:2012 recommends that the classification of ground condition should be S_A, S_B, S_C, S_D and S_E dependent

on geotechnical site characteristics (e.g., shear wave velocity, SPT number of blow counts, undrained shear strength) for the ground up to 30 m of depth or to moderate rock. According to TCVN 9386:2012, the seismic site classification in Ho Chi Minh City can be classified by S_D, which comprises mostly cohesive soil layers or a few granular soil layers adjacent to cohesive soil layers (i.e., average shear wave velocity at 30 m of depth is lower than 180 m/s, and SPT number of blow counts is lower than 15).

Figure 2 presents the SPT number of blow counts (N_{60}) and corrected SPT values of $(N_1)_{60}$ of 24 boreholes at each district in Ho Chi Minh City. The corrected SPT values of $(N_1)_{60}$ are converted from N_{60} using the overburden correction factor C_N proposed by Liao and Whitman (1986). It is noted that field experience during past earthquakes (Iwasaki et al., 1984; Youd et al., 2001) stated that liquefaction primarily occurs at a depth of less than 20 m with respect to granular soil stratigraphy. Therefore, several boreholes in some districts are mostly encountered as clay minerals or organic silt within a depth of 20 m. The (N_{60}) and $(N_1)_{60}$ values are expected to be very low (i.e., lower than 5). It is assumed that there is no liquefaction will occur in these areas. It is seen that data with the grey color in Figure 2 reveals these kinds of boreholes, including District 2, District 7, District 8, District 9, Binh Chanh District, Binh Tan District, Binh Thanh District, Cu Chi District, Nha Be District, Can Gio, and Hoc Mon District. Moreover, below the depth of 50 m, moderately stiff soil layers (i.e., mainly $N_{60} > 50$) have been considered as the bedrock to apply the input ground motion for further analysis.

Key input parameters for the equivalent linear analysis are the maximum shear modulus (G_{max}) or shear wave velocity (V_s), which are determined using the formula proposed by Seed et al. (1986).

$$G_{max} = 21{,}7.K_{2max}.P_a.\left(\frac{\sigma_m^{'}}{P_a}\right)^{0.5} \quad (16)$$

$$K_{2max} = 20.(N_1)_{60}{}^{0.333} \quad (17)$$

where, G_{max} is the maximum shear modulus, K_{2max} is the number of shear moduli, P_a is the atmospheric pressure ($P_a \approx 100$ kPa), σ'_m is the vertical effective stress, $(N_1)_{60}$ is the corrected SPT number of blow counts.

To perform the effective stress analysis, the $(N_1)_{60}$ is required as input. The other parameters necessary for the analysis can be determined using formulas presented in Tables 1 for the Finn-Byrne model and Table 2 for the UBCSAND model, respectively. The Finn-Byrne and UBCSAND model were designated for use with sand, silty sand, and sandy gravel strata. Meanwhile, the Mohr-Coulomb model with elastic-perfect plasticity was designated for the clay or clayey silt layers, which are considered to be soil layers that do not undergo liquefaction. It was assumed that the permeability (k) in likely clay layers would have a low value of 10^{-8} m/s. By this assumption, the values for the shear modulus (G), bulk modulus (B), cohesion (c'), and friction angle (φ') were estimated to be $G = 10^5$ kPa, $B = 3\times10^5$ kilopascals, $c' = 100$ kPa, and $\varphi' = 20°$, respectively. As noted by Das and Sobhan (2013), the permeability of fine sand tends to range from 10^{-4} to 10^{-5} m/s, whereas, for sandy gravel, it can range from 10^{-3} to 10^{-4} m/s. In the case of silty sand, the permeability typically falls between 10^{-5} and 10^{-6} m/s. In this study, effective stress analyses were conducted with permeabilities of 10^{-5} m/s for sand. It was assumed that the initial saturation values prior to the earthquake were 99%, which would lead to a substantial increase in excess pore water pressure.

Other information on geotechnical data, such as bulk density (γ_b), dry density (γ_d), fine content (FC), corresponding particle size (D_{50}), water content (w), liquid limit (LL), and plastic index (PI), is available in the database (Doan, 2023). The data is a compilation of both in situ and laboratory test results at the observed boreholes in Ho Chi Minh City.

4. INPUT GROUND MOTION

Given the lack of recorded motions in the Ho Chi Minh City area, a similar approach to Nguyen et al. 2020) has been adopted in this study. A total of 12 earthquake events are selected with respect to similar characteristics to those likely occurred in Vietnam. It is worth extracting these recorded motions from the NGA-West2 database (https://ngawest2.berkeley.edu/) with regard to the following characteristics:

- Surface moment magnitude (M_w) in a range of [5.5 – 7.5].
- Rupture distance (R_{rup}) in a range of [0.92 – 85.17] km.
- V_{s30} in a range of [760 – 1500] m/s.

The detailed characteristics of selected earthquake events are shown in Table 3.

Figure 3 illustrates a series of response spectra of selected earthquake events from the NGA-West2 database. Two horizontal components of the recorded motions (i.e., North-West or South-East directions) are shown in Figure 3 since shear wave motions might cause more catastrophic damages than vertical component. It is concluded that the recorded motion in the North-West horizontal of the Kobe earthquake occurred in 1995 has been selected as the input ground motion for further analysis since the response spectra produced by this event was recorded up to 0.92 g at 1.2 s and with many slightly lower spikes during the period.

Figure 4(a) shows the target response spectra of 24 districts in Ho Chi Minh City calculated based on TCVN 9386:2012. It is noted that the fundamentals of the method in TCVN 9386:2012 come from Eurocode 8 (Code, 2005) and it is applicable to local Vietnamese soil conditions. A detailed description and calculation guidelines of response spectra can be found in (Nguyen et al., 2020). As mentioned in Section 3, the seismic site classification S_D has been used to compile target

response spectra for 24 districts in Ho Chi Minh City. Subsequently, the North-West horizontal motion from Figure 3 (representing the Kobe earthquake of 1995) was used to match the target response spectra of 24 districts in Ho Chi Minh City by an open-source code known as REQPY (Montejo, 2021). The results of the matching are presented in Figure 4(b). It is seen that the matching response spectra are consistent with the target response spectra in accordance with TCVN 9386:2012 (Vietnam National Code, 2012).

Figure 5 shows a comparison between the original motion of the 1995 Kobe earthquake and the matched motion using the REQPY (Montejo, 2021) at District 3, Ho Chi Minh City in accordance with TCVN 9386:2012. In general, there is a similarity between the two acceleration spectra with peaks at corresponding time intervals. The peaks in the original motion are nearly twice as long as those in the matched motion.

Similarly, the acceleration time history of each matching motion was conducted for each district respectively. The resulting matched acceleration spectra were then used as input ground motion at the base of the 1D column soil model for equivalent linear analysis, effective stress analysis using the Finn-Byrne model, and the UBCSAND model. It is noted that the simplified method solely uses the *PGA* from Table 3 corresponding to the location of the observed borehole and surface magnitude of the earthquake (i.e., assumed $M_w = 5.5$ for the potential earthquake that might occur in Ho Chi Minh City) for the liquefaction assessment analysis.

5. RESULTS AND DISCUSSIONS

Figure 6 shows the detailed numerical results of alternative analyses at various depths, including the simplified method, equivalent linear analysis, loosely-coupled effective stress

394 analysis using the Finn-Byrne model, and fully-coupled effective stress analysis using the
395 UBCSAND model, for the liquefaction evaluation of the soil profile in District 3, Ho Chi Minh
396 City. Due to the large amount of data from the analysis results of various methods for multiple
397 boreholes in Ho Chi Minh City, it is not feasible to display all detailed results in this study.
398 Consequently, the specific outcomes of the borehole located in District 3 were selected as the
399 representative example to contrast the results of analysis obtained from alternative approaches.
400 This will enable a comprehensive assessment of the merits and drawbacks of the methods.

401 Figure 6(a) depicts the distribution of the input data, which are the SPT number of blow
402 counts N_{60} and the corrected SPT number of blow counts $(N_1)_{60}$, along the depth. Generally, $(N_1)_{60}$
403 is higher than N_{60} in the depth range of 0-10 m, however, the trend reverses below 10 m depth.
404 This could be explained by the increasing overburdened stress in the soil profile. The $(N_1)_{60}$ is the
405 key input parameter for further analyses.

406 Figure 6(b) shows the *CRR* and *CSR* results extracted from various methods versus the
407 depth of the soil profile. Based on the input data $(N_1)_{60}$ from the SPT, the *CRR* for the ground
408 subjected to an earthquake with magnitude $M_w = 5.5$ was calculated using Equation (6) (Boulanger
409 and Idriss 2014) and adjusted from $M_w = 7.5$ to Mw = 5.5 according to Equation (9). As depicted,
410 the *CRR* values are primarily within the range of 0.15-0.2 at depths between 10-42 m. In the depths
411 of 0-5 m and 42-50 m, the soil layer is clay, hence, the default *CRR* value is set to 2. According to
412 the simplified analysis method, the *CSR* ratio is calculated using Equation (2) as proposed by (Seed
413 and Idriss, 1971). Based on the equivalent linear analysis method, the *CSR* is estimated from the
414 SHAKE91 program. For effective stress analysis, the *CSR* can be directly obtained from the
415 UBCSAND and Finn-Byrne model analysis results. As shown in Figure 6(b), there is a consistency
416 between the *CSR* calculated from the analyses. It has been determined that the *CSR* estimated by

417 the equivalent linear analysis method is only slightly higher than that obtained from the simplified
418 method and falls within a range of [0.15-0.2]. Meanwhile, *CSR* predictions from effective stress
419 analysis using the Finn-Byrne and the UBCSAND models are significantly higher than the
420 predicted values from the simplified method and equivalent linear analysis, ranging from 0.3 to
421 0.6. Furthermore, the UBCSAND model predicts the highest *CSR* values and shows a close
422 similarity to the *CSR* predictions from the Finn-Byrne model, with decreasing *CSR* values as the
423 depth increases.

424 Figure 6(c) presents the distribution of the *FS* to liquefaction as calculated from various
425 methods with respect to the depth of the soil profile in District 3, Ho Chi Minh City. In general,
426 the soil profile does not demonstrate susceptibility to liquefaction when *FS* is greater than 1, as
427 predicted by the simple analysis method and the equivalent linear analysis. However, the effective
428 stress analysis using the UBCSAND and Finn-Byrne models indicates that the soil profile liquefies
429 at depths ranging from 12-42 m. The distribution of *FS* with respect to the depth is computed from
430 the methods that exhibit coherence, in which the predicted values from the UBCSAND model are
431 the lowest, followed by the values from the Finn-Byrne model, SHAKE91 program, and the
432 simplified method. It should be noted that there is a slight difference in the results from the
433 UBCSAND and Finn-Byrne models.

434 Figure 6(d) compares the maximum shear strains (γ_{max}) along the depth computed from the
435 four methods. The γ_{max} computed from the simplified method (i.e., (Boulanger and Idriss, 2014))
436 is significantly higher than that obtained from the linear equivalent analysis method (i.e.,
437 SHAKE91 program). On the other hand, the γ_{max} computed from the effective stress analysis (i.e.,
438 UBCSAND and Finn-Byrne models) are relatively smaller compared to those obtained from the
439 simplified method. Especially, at a depth of 40-50 m, the results obtained from the effective stress

analyses are much higher than those from the other two methods. The reason is due to the boundary conditions at the bottom of the 1D site response model in the simplified method and equivalent linear analysis being fixed, while input ground motion at the bottom of the model is allowed in the horizontal direction in the effective stress analyses.

Figure 6(e) presents a comparison of *LPI* values, as determined by different analyses. Typically, when using effective stress methods (i.e., UBCSAND and Finn-Byrne models), the liquefaction potential is higher for soil layers situated above 10 m in depth. By Iwasaki et al.'s (Iwasaki et al., 1984) classification of liquefaction hazards, the *LPI* value of $5 \leq LPI \leq 15$ indicates a high risk of liquefaction at shallow depths. The *LPI* at ground level is the sum of *LPI* values for each soil layer from the surface to a depth of 20 m and is greater than 0 when the *FS* is less than 1. It should be noted that the *LPI* calculated using effective stress analyses is significantly greater than that obtained using the other two methods. On the other hand, both the simplified method and equivalent linear analysis result in *LPI* values that are almost equal to zero.

Figures 8(f-h) depict the results of four different liquefaction assessment methods for maximum volumetric strain (ε_v), *LSN*, and ground settlement (*S*) at various depths. As the ε_v cannot be directly calculated by the equivalent linear analysis method, its predictions from this method are not presented in the charts. In general, there is a similarity in volumetric strain results between the simplified method and the UBCSAND model, leading to a minimal difference in LSN between the two methods. The reason is that *LSN* is an integral function of volumetric strain and depth. However, the Finn-Byrne model shows significantly lower results of ε_v and *LSN* compared to the simplified method and the UBCSAND model. Herein, the ε_v is the large value at a depth of 10-35 m compared to other depths, leading to an estimated *LSN* of approximately 1.5 at the ground surface based on the results of the simplified method and the UBCSAND model. The UBCSAND

model produces the highest ground settlement value, approximately 6 cm, followed by the simplified method, which performs a settlement of nearly 3 cm, and lastly, the Finn-Byrne model analysis, which provides the smallest ground settlement value, at approximately 0.3 cm.

Figure 6(i) reveals the excess pore pressure ratio (R_u) as a function of depth, as computed by the Finn-Byrne and the UBCSAND effective stress analyses. The R_u derived from the Finn-Byrne model is substantially lower than that obtained from the UBCSAND model. The R_u reaches a value of up to 0.5 at a specific depth of around 10 m, implying that liquefaction may take place at depths ranging from 10 to 40 m.

A general explanation for the results in Figure 6 can be provided as follows. Since the UBCSAND model takes into account both the behavior of the soil skeleton and the development of pore water pressure within the plasticity framework, its estimations of liquefaction are the most accurate and lead to the smallest *FS*. On the other hand, the Finn-Byrne model employs empirical relationships to simulate pore pressure generation and shear-induced volumetric strain, resulting in significantly lower predictions for *R*u, ε_v, *LSN*, and ground settlement (*S*) compared to those generated by the UBCSAND model. However, the predictions for *CSR*, *FS*, γ_{max}, and *LPI* do not show significant differences compared to those obtained from the UBCSAND model. When performing the simplified method, using only the *PGA* and *M*w of the earthquake for the entire calculation produces the highest *FS*, which is also the most conservative outcome. Although the equivalent linear analysis employs real-time acceleration data, it is still fundamentally based on total stress, which neglects the interplay between the soil structure and the pore water pressure, and only accounts for the linear elastic phase of the material. As a result, the computed results from the equivalent linear method fall in between those obtained from the other three methods.

Figure 7 is a comparison of the *LPI* estimated from the simplified method, equivalent linear

analysis, and effective stress analysis using the Finn-Byrne model, and UBCSAND model, respectively. As mentioned, the districts with the ground mainly comprises clay deposits are considered non-liquefaction, including District 2, District 7, District 8, District 9, Binh Chanh, Nha Be, Can Gio, Binh Tan, Cu Chi, Binh Thanh, and Hoc Mon. Iwasaki et al. (Iwasaki et al., 1984) proposed a classification of five levels based on the value of *LPI* as shown in Figure 7. Generally, the liquefaction potential, as assessed by the *LPI*, is found to be highest when calculated using the UBCSAND model, followed by the Finn-Byrne model, SHAKE91 program, and the simplified method, in descending order. The liquefaction potential in the observed districts is found to be very low (i.e., *LPI* = [0-2]) when assessed using the simplified method. However, a moderate liquefaction potential (i.e., *LPI* = [2-5]) is observed in District 1 and District 12 when the equivalent linear analysis method is employed. There are slight differences in the assessment of the liquefaction potential using the Finn-Byrne and UBCSAND models. According to the results from the UBCSAND and Finn-Byrne models, Thu Duc exhibits a low liquefaction potential (i.e., *LPI* = [0-2]). In contrast, districts 1, 5, 10, 11, 12, and Tan Phu demonstrate a very high potential for liquefaction (i.e., *LPI* > 15), while districts 4, Tan Binh, and Go Vap present a moderate potential for liquefaction (i.e., *LPI* = [5-15]). The UBCSAND model predicts that Districts 3 and 6 have a very high liquefaction potential, while the Finn-Byrne model predicts that they have a high and moderate potential, respectively.

Figure 8 depicts a comparison between the estimated *LSN* values obtained from the simplified method, the Finn-Byrne model, and the UBCSAND model. It should be noted that the equivalent linear analysis method cannot capture the volumetric strain, and therefore the result from this method was not included in the figure. It is seen that all the observed districts exhibit a significantly low probability of liquefaction-induced damage (i.e., *LSN* = [0-10]), according to the

509 results of the effective stress analysis (i.e., Finn-Byrne and UBCSAND models). On the other hand,
510 the simplified method predicts a minor probability of liquefaction-induced damage (i.e., *LSN* =
511 [10-30]) in districts 1 and 12, and little possibility of damage due to liquefaction (i.e., *LSN* = [0-
512 10]) in other locations.

513 Figure 9 demonstrates the maps of liquefaction-induced surface ground settlement
514 estimated from alternative approaches. As previously mentioned, the figure does not show the
515 result from equivalent linear analysis because this method is incapable of predicting shear-induced
516 volumetric strain. It is seen that the ground surface settlement resulting from liquefaction is
517 observed to be minimal, ranging from 0 to 2 cm, when using the Finn-Byrne model. In contrast,
518 the settlement results are much higher, ranging from 2 to 6 cm for the observed boreholes in Ho
519 Chi Minh City. The simplified method predicts the highest settlement in Districts 1 and 12, ranging
520 from 8 to 10 cm, followed by S = 4-6 cm in Districts 3 and 4, and S = 0-2 cm in the remaining
521 districts.

522

523 **6. CONCLUSIONS**

524

525 Soil liquefaction-induced settlement can significantly impact the structure of buildings, roads,
526 bridges, and ports during seismic activity. In this study, four analysis methods were used to
527 evaluate the liquefaction potential of soil: simplified method adopting (Boulanger and Idriss,
528 2014)'s liquefaction triggering relationship, equivalent linear analysis using SHAKE91 program,
529 effective stress analysis using the Finn-Byrne model and UBCSAND model, respectively. This
530 analysis utilized the SPT data from 24 districts around Ho Chi Minh City. The seismic loading data
531 is extracted from the NGA-West2 database, which has similar characteristics to those likely

532 occurred in Vietnam in the past, and they are matched to target response spectra compiled from
533 TCVN 9386:2012. The computed results from the four analyses were compared together to
534 demonstrate the advantages and accuracy of each method. The maps of *LPI*, *LSN*, and surface
535 ground settlement due to seismic loading are first proposed for Ho Chi Minh City stratigraphy.
536 Some conclusions can be drawn as follows:

537 • The simplified method possesses the advantage of rapid computation, simplicity, and solely
538 using the *PGA* a_{max} and earthquake magnitude M_w throughout the analysis process. The
539 results from this method exhibit the highest level of *FS*, the lowest *LPI*, the most *LSN*, and
540 the most pronounced surface ground settlement This method is employed to perform an
541 initial evaluation of the liquefaction potential at a designated site. it should not be employed
542 to calculate soil settlement or LSN due to its excessively conservative results in comparison
543 to actuality.

544 • The equivalent linear analysis method involves iterative analyses that gradually reduce the
545 soil shear modulus and damping ratio to simulate its nonlinear behavior. In this study, the
546 SHAKE91 program was utilized for the equivalent linear analysis. Despite utilizing the
547 acceleration time history for analysis, this method still employs the total stress approach,
548 neglecting the effects of increased pore pressure due to liquefaction. Thus, the results
549 obtained from the analysis using the equivalent linear analysis method are considered to be
550 safer than those obtained by effective stress analysis, but more hazardous than those
551 obtained by simple analysis. Furthermore, the limitation of this method lies in its
552 incapability to compute volumetric strain during vibration, thereby making it unable to
553 predict soil settlement and the *LSN*.

554 • The effective stress analysis method is considered the most reliable means of assessing soil

liquefaction due to its comprehensive consideration of the behavior of both the soil skeleton and pore water, as well as the elastic-plastic model of the soil material. However, the model parameters are relatively complex, requiring users to have experience in selecting input data and taking a considerable amount of time for each analysis. The present study employs the UBCSAND model for the fully-coupled effective stress analysis and the Finn-Byrne model for the loosely-coupled effective stress analysis, using real-time acceleration data from earthquake ground motion throughout the analysis. The UBCSAND model is capable of producing the most accurate liquefaction predictions due to its ability to account for both the behavior of the soil structure and the development of pore water pressure within a plasticity framework, which leads to lower *FS*. In contrast, the Finn-Byrne model employs empirical relationships to simulate shear-induced volumetric strain and pore pressure generation, resulting in lower estimates of R_u, ε_v, *LSN*, and ground settlement (*S*) compared to those predicted by the UBCSAND model. However, the predictions for *CSR*, *FS*, γ_{max}, and *LPI* do not show any significant differences when compared to those obtained from the UBCSAND model.

ACKNOWLEDGEMENT

The authors have a grateful thank to Industrial University of Ho Chi Minh City for the financial support for the research fund, grant number 21.2XD02.

DATA AVAILABILITY STATEMENT:

The data in this study is available at http://dx.doi.org/10.17632/4xbt9h34sb.1. Some models, or code generated or used during the study are available from the corresponding author by request.

REFERENCES

Andrus, R.D., Stokoe II, K.H., 2000. Liquefaction resistance of soils from shear-wave velocity. Journal of geotechnical and geoenvironmental engineering 126, 1015–1025.

Beaty, M.H., Byrne, P.M., 2011. UBCSAND Constitutive Model, Version 904aR [WWW Document]. Itasca UDM Web Site. URL https://www.itascacg.com/software/udm-library/ubcsand (accessed 12.20.19).

Beaty, M.H., Perlea, V.G., 2011. Several observations on advanced analyses with liquefiable materials, in: Proceedings of the 31st Annual USSD Conference and 21st Conference on Century Dam Design-Advances and Adaptations. pp. 1369–1397.

Boulanger, R., Idriss, I.M., 2014. CPT and SPT Based Liquefaction Triggering Procedures. Report No. UCD/CGM-14/01. University of California at Davis, Davis, California.

Boulanger, R.W., Ziotopoulou, K., 2015. PM4Sand (Version 3): A sand plasticity model for earthquake engineering applications. Center for Geotechnical Modeling Report No. UCD/CGM-15/01, Department of Civil and Environmental Engineering, University of California, Davis, Calif.

Byrne, M.P., 1991. A cyclic shear-volume coupling and pore pressure model for sand, in: Proceedings of Second International Conference on Recent Advances in Geotechnical Engineering and Soil Dynamics. University of Missouri-Rolla, St. Louis, Missouri, pp. 47–55.

Byrne, P.M., Park, S.-S., Beaty, M., Sharp, M., Gonzalez, L., Abdoun, T., 2004. Numerical modeling of liquefaction and comparison with centrifuge tests. Canadian Geotechnical Journal 41, 193–211.

Cetin, K.O., Seed, R.B., der Kiureghian, A., Tokimatsu, K., Harder Jr, L.F., Kayen, R.E., Moss, R.E.S., 2004. Standard penetration test-based probabilistic and deterministic assessment of seismic soil liquefaction potential. Journal of geotechnical and geoenvironmental engineering 130, 1314–1340.

Chi, T.N., others, 2017. Liquefaction possibilityof soil layers during earthquake in Hanoi. GEOMATE Journal 13, 148–155.

Code, P., 2005. Eurocode 8: Design of structures for earthquake resistance-part 1: general rules, seismic actions and rules for buildings. Brussels: European Committee for Standardization.

Das, B.M., Sobhan, K., 2013. Principles of geotechnical engineering. Cengage learning.

Doan, N.-P., 2023. Liquefaction assessment of Ho Chi Minh City Stratigraphy [WWW Document]. Mendeley Data, V1. URL http://dx.doi.org/10.17632/4xbt9h34sb.1 (accessed 2.19.23).

Doan, N.-P., 2021. Application of UBCSAND2 Constitutive Model for PostLiquefaction Assessment. Kyungpook National University.

Doan, N.P., Park, S.S., Lee, D.E., 2020a. Assessment of Pohang earthquake-induced liquefaction at Youngil-man port using the UBCSAND2 model. Applied Sciences (Switzerland) 10, 5424. https://doi.org/10.3390/APP10165424

Doan, N.P., Woo, S.W., Hou, Y.L., Park, S.S., 2020b. Finite element simulation of water content-influenced progressive failure of sensitive clays, in: In Proc., CIGOS 2019,

Innovation for Sustainable Infrastructure. Springer, Singapore, Hanoi, Vietnam, pp. 841–846. https://doi.org/10.1007/978-981-15-0802-8_134

Finn, W.D., 1985. Aspects of constant volume cyclic simple shear, in: Advances in the Art of Testing Soils under Cyclic Conditions. pp. 74–98.

Galavi, V., Petalas, A., Brinkgreve, R.B.J., 2013. Finite element modelling of seismic liquefaction in soils. Geotechnical Engineering Journal of the SEAGS & AGSSEA, 44 (3), 2013.

Golesorkhi, R., 1989. Factors influencing the computational determination of earthquake-induced shear stresses in sandy soils. University of California, Berkeley.

Hua, T.T., Nguyen, N.P., Nguyen, V.C., 2017. Analysis of liquefaction capacity in sand foundation for the construction of coastal areas in Binh Dinh province. Vietnam Geotechnical Journal 21, 51–61.

Hung, T.V., 2012. Study on earthquake ground motion prediction and its application to structural response of bridge in Vietnam.

Idriss, I.M., 1999. An update to the Seed-Idriss simplified procedure for evaluating liquefaction potential. Proc., TRB Worshop on New Approaches to Liquefaction, Pubbl. n. FHWA-RD-99-165, Federal Highway Administation.

Idriss, I.M., Boulanger, R.W., 2008. Soil liquefaction during earthquakes. Earthquake Engineering Research Institute.

Idriss, I.M., Seed, H.B., 1968. Seismic response of horizontal soil layers. Journal of the Soil Mechanics and Foundations Division 94, 1003–1031.

643 Idriss, I.M., Sun, J.I., 1992. SHAKE91: A computer program for conducting equivalent linear
644 seismic response analyses of horizontally layered soil deposits. University of California,
645 Davis 13.
646 Itasca Consulting Group Inc., 2011. FLAC–Fast Lagrangian Analysis of Continua, version 7.0
647 [WWW Document]. URL https://www.itascacg.com/software/downloads/flac-7-00-update
648 (accessed 12.20.19).
649 Iwasaki, T., Arakawa, T., Tokida, K.-I., 1984. Simplified procedures for assessing soil
650 liquefaction during earthquakes. International Journal of Soil Dynamics and Earthquake
651 Engineering 3, 49–58.
652 Kayen, R., Moss, R.E.S., Thompson, E.M., Seed, R.B., Cetin, K.O., Kiureghian, A. der, Tanaka,
653 Y., Tokimatsu, K., 2013. Shear-wave velocity–based probabilistic and deterministic
654 assessment of seismic soil liquefaction potential. Journal of Geotechnical and
655 Geoenvironmental Engineering 139, 407–419.
656 Le, T.-T., Park, S.-S., Woo, S.-W., 2022a. Cyclic Response and Reconsolidation Volumetric
657 Strain of Sand under Repeated Cyclic Shear Loading Events. Journal of Geotechnical and
658 Geoenvironmental Engineering 148, 4022109.
659 Le, T.-T., Park, S.-S., Woo, S.-W., Tran, L., 2022b. Cyclic response and post-cyclic settlement
660 of sand experiencing repeated earthquakes, in: CIGOS 2021, Emerging Technologies and
661 Applications for Green Infrastructure: Proceedings of the 6th International Conference on
662 Geotechnics, Civil Engineering and Structures. pp. 1015–1023.
663 Liao, S.S.C., Whitman, R. v, 1986. Overburden correction factors for SPT in sand. Journal of
664 geotechnical engineering 112, 373–377.

Martin, G.R., Finn, W.D.L., Seed, H.B., 1975. Fundamentals of Liquefaction under Cyclic Loading. Journal of the Geotechnical Engineering Division (ASCE) 101, 423–438.

Montejo, L.A., 2021. Response spectral matching of horizontal ground motion components to an orientation-independent spectrum (RotDnn). Earthquake Spectra 37, 1127–1144.

Moss, R.E., Seed, R.B., Kayen, R.E., Stewart, J.P., der Kiureghian, A., Cetin, K.O., 2006. CPT-based probabilistic and deterministic assessment of in situ seismic soil liquefaction potential. Journal of Geotechnical and Geoenvironmental Engineering 132, 1032–1051.

Ngo, T., Nguyen, M.D., Nguyen, D.B., 2008. Review of the current Vietnamese earthquake design code. Electronic Journal of Structural Engineering 32–41.

Nguyen, B.-P., Doan, N.-P., Kim, Y.-T., 2021a. Vertical stress distribution on stiffened deep cement mixing column under embankment load, in: Challenges and Innovations in Geomechanics: Proceedings of the 16th International Conference of IACMAG-Volume 2 16. pp. 825–832.

Nguyen, B.-P., Ngo, C.P., Tran, T.D., Bui, X.C., Doan, N.-P., 2022. Finite element analysis of deformation behavior of deep excavation retained by Diagram Wall in Ho Chi Minh City. Indian Geotechnical Journal 52, 989–999.

Nguyen, B.-P., Pradhan, A.M.S., Nguyen, T.H., Doan, N.-P., Nguyen, V.-Q., Huynh, T.-C., 2021b. Large-strain consolidation analysis of PVD-installed soft soil considering the discharge capacity variation according to depth and time. Eng Comput (Swansea) 38, 1652–1676.

Nguyen, H.B.K., Rahman, M.M., Fourie, A.B., 2018. Characteristic behavior of drained and undrained triaxial compression tests: DEM study. Journal of Geotechnical and Geoenvironmental Engineering 144, 4018060.

Nguyen, H.B.K., Rahman, M.M., Fourie, A.B., 2017. Undrained behaviour of granular material and the role of fabric in isotropic and K 0 consolidations: DEM approach. Géotechnique 67, 153–167.

Nguyen, T., Ly, K.-D., Nguyen-Thoi, T., Nguyen, B.-P., Doan, N.-P., 2022. Prediction of axial load bearing capacity of PHC nodular pile using Bayesian regularization artificial neural network. Soils and Foundations 62, 101203.

Nguyen, T.-K., Nguyen, V.-Q., 2022. One-dimensional Site Response Analysis and Liquefaction Evaluation of Can Tho City, Vietnam. Engineering, Technology & Applied Science Research 12, 9676–9679.

Nguyen, V.-Q., Aaqib, M., Nguyen, D.-D., Luat, N.-V., Park, D., 2020. A site-specific response analysis: a case study in Hanoi, Vietnam. Applied Sciences 10, 3972.

Nhung, B.T., Phuong, N.H., Nam, N.T., 2017. Assessment of earthquake-induced ground liquefaction susceptibility for Hanoi city using geological and geomorphologic characteristics. Science of the Earth 39, 139–154.

Nhung, B.T., Phuong, N.H., Nam, N.T., others, 2018. Assessment of earthquake-induced liquefaction hazard in urban areas of Hanoi city using LPI-based method. Science of the Earth 40, 78–96.

Nu, N.T., Duong, N.T., Son, B.T., 2021. Assessment of Soil Liquefaction Potential Based on SPT Values at Some Ground Profiles in the North Central Coast of Vietnam. Iraqi Journal of Science 2222–2238.

Park, S.S., Doan, N.P., Jeong, S.W., 2020. Numerical simulation of water content dependent undrained shear strength of clays. Marine Georesources and Geotechnology 38, 621–632. https://doi.org/10.1080/1064119X.2019.1608604

711 Park, S.-S., Doan, N.-P., Nong, Z., 2020. Numerical prediction of settlement due to the Pohang
712 earthquake. Earthquake Spectra. https://doi.org/10.1177/8755293020957345
713 Park, S.S., Nong, Z.Z., Doan, N.P., 2021. Constitutive Modeling of Principal Stress Rotation
714 associated with Sand under Simple Shear Loading. Int J Numer Anal Methods Geomech.
715 Park, S.-S., Tran, D.-K.-L., Doan, N.-P., 2021. Numerical Simulation of the Effect of Void
716 Direction and Volume on the Strength of Cemented Soil. International Journal of
717 Geomechanics 22, 4022001.
718 Pham, T.M., Dai Vo, N., 2014. Estimation of liquefaction of sandy soil in District 7, HCMC,
719 Vietnam. VNUHCM Journal of Science and Technology Development 17, 40–44.
720 Puebla, H., Byrne, P.M., Phillips, R., 1997. Analysis of CANLEX liquefaction embankments:
721 prototype and centrifuge models. Canadian Geotechnical Journal 34, 641–657.
722 https://doi.org/10.1139/cgj-34-5-641
723 Rahman, M.M., Nguyen, H.B.K., Fourie, A.B., Kuhn, M.R., 2021. Critical state soil mechanics
724 for cyclic liquefaction and postliquefaction behavior: DEM study. Journal of Geotechnical
725 and Geoenvironmental Engineering 147, 4020166.
726 Robertson, P.K., Shao, L., 2010. Estimation of seismic compression in dry soils using the CPT,
727 in: Fifth International Conference on Recent Advances in Geotechnical Earthquake
728 Engineering and Soil Dynamics, San Diego, CA, USA.
729 Schnabel, P.B., 1972. SHAKE, a computer program for earthquake response analysis of
730 horizontally layered sites. Report No. EERC 72-12, University of California, Berkeley.
731 Seed, H.B., Idriss, I.M., 1971. Simplified procedure for evaluating soil liquefaction potential.
732 Journal of Soil Mechanics & Foundations Div.

Seed, H.B., Idriss, I.M., 1970. Soil moduli and damping factors for dynamic analysis. Report No. EERC 70-10. University of California, Berkeley.

Seed, H.B., Wong, R.T., Idriss, I.M., Tokimatsu, K., 1986. Moduli and damping factors for dynamic analyses of cohesionless soils. Journal of geotechnical engineering 112, 1016–1032.

Tran, N.-L., Aaqib, M., Nguyen, B.-P., Nguyen, D.-D., Tran, V.-L., Nguyen, V.-Q., 2021. Evaluation of seismic site amplification using 1D site response analyses at Ba Dinh Square Area, Vietnam. Advances in Civil Engineering 2021, 1–11.

van Ballegooy, S., Malan, P., Lacrosse, V., Jacka, M.E., Cubrinovski, M., Bray, J.D., O'Rourke, T.D., Crawford, S.A., Cowan, H., 2014. Assessment of liquefaction-induced land damage for residential Christchurch. Earthquake spectra 30, 31–55.

Vietnam National Code, 2012. TCVN 9386:2012 0 - Design of Structures for Earthquake Resistances;

Youd, T.L., Idriss, I.M., Andrus, R.D., Arango, I., Castro, G., Christian, J.T., Dobry, R., Finn, W.D.L., Harder, L.F., Hynes, M.E., Ishihara, K., Koester, J.P., Liao, S.S.C., Marcuson, W.F., Martin, G.R., Mitchell, J.K., Moriwaki, Y., Power, M.S., Robertson, P.K., Seed, R.B., Stokoe, K.H., 2001. Liquefaction resistance of soils: Summary report from the 1996 NCEER and 1998 NCEER/NSF workshops on evaluation of liquefaction resistance of soils. Journal of Geotechnical and Geoenvironmental Engineering. https://doi.org/10.1061/(ASCE)1090-0241(2001)127:10(817)

Zhang, G., Robertson, P.K., Brachman, R.W.I., 2002. Estimating liquefaction-induced ground settlements from CPT for level ground. Canadian Geotechnical Journal 39, 1168–1180.

756

LIST OF TABLES AND FIGURES

780 effective stress analysis (Finn-Byrne model), and (d) fully-coupled effective stress analysis
781 (UBCSAND model) based on available SPT database and target response spectra to TCVN
782 9386:2012
783 **Figure 8.** Distribution of liquefaction severity number (*LSN*) interpolated across the land of Ho
784 Chi Minh metropolitan city using alternative methods: (a) simplified method (Idriss and Boulanger
785 (Boulanger and Idriss, 2014)), (b) loosely-coupled effective stress analysis (Finn-Byrne model),
786 and (c) fully-coupled effective stress analysis (UBCSAND model) based on available SPT
787 database and target response spectra to TCVN 9386:2012
788 **Figure 9.** Distribution of surface ground settlement (*S*) interpolated across the land of Ho Chi
789 Minh metropolitan city using alternative methods: (a) simplified method (Idriss and Boulanger
790 (Boulanger and Idriss, 2014)), (b) loosely-coupled effective stress analysis (Finn-Byrne model),
791 and (c) fully-coupled effective stress analysis (UBCSAND model) based on available SPT
792 database and target response spectra to TCVN 9386:2012.
793

794 **Table 1.** Input parameters of Finn-Byrne model

Parameters	**Generic parameters**	
	Function	**Values**
$(N_1)_{60,cs}$	Normalized, corrected SPT blow counts	Varies
C_{Dr}	Correlation factor between $(N_1)_{60}$ and D_r	Constant=46
D_r	Relative density	$[(N_1)_{60}/C_{Dr}]^{0.5}$
ϕ	Friction angle	33˚
Ψ	Dilation angle	0˚
c	Cohesion	0 kPa
t	Tension cutoff	0 kPa
G	Shear modulus	$21.7\times20\times(N_1)_{60}^{0.333}$
B	Bulk modulus	$0.7\times G$
ff_c1	Constant C_1	$8.7\times(N_1)_{60}^{-1.25}$
ff_c2	Constant C_2	$0.4/C_1$
ff_latency	Minimum number of timesteps between reversals	1000000
ff_switch	Factor of switching between Byrne or Martin's cyclic volumetric-shear strain relationship	1

795 Note: σ'_{v0} = initial vertical effective stress, and P_{atm} = atmospheric pressure (~100 kPa).

796 **Table 2**. Input parameters of UBCSAND model

Parameters	Generic parameters	
	Function	**Values**
$(N_1)_{60,cs}$	Normalized, corrected SPT blow counts	Varies
C_{Dr}	Correlation factor between $(N_1)_{60}$ and D_r	Constant
D_r	Relative density	$[(N_1)_{60}/C_{Dr}]^{0.5}$
ϕ_{cv}	Constant volume friction angle	33˚
ϕ_f	Peak friction angle	$\phi_{cv}+(N_1)_{60}/10+\max(0, ((N_1)_{60}-15)/5)$
k_G^e	Elastic shear modulus number	$21.7\times20\times(N_1)_{60}^{0.333}$
k_B^e	Elastic bulk modulus number	$0.7\times k_G^e$
k_G^p	Plastic shear modulus number	$k_G^e\times(N_1)_{60}^2\times0.003+100$
m_e	Elastic shear exponent	0.5
n_e	Elastic bulk exponent	0.5
n_p	Plastic shear exponent	0.4
R_f	Failure ratio	$\min(1.1\times(N_1)_{60}^{-0.15}, 0.99)$
a	Factor for *hfac1* calculation	$1.05-0.03\times(N_1)_{60}+0.04\times[(N_1)_{60}]^2-0.000185\times[(N_1)_{60}]^3+2.92E-6\times[(N_1)_{60}]^4$
b	Factor for *hfac1* calculation	$1.0/\{-0.424-0.259\times(N_1)_{60}+0.00763\times[(N_1)_{60}]^2\}$
hfac1	Factor of primary hardener	$a\times(\sigma'_{v0}/P_{atm})^b$
hfac2	Factor of secondary hardener	1.0
hfac3	Factor of dilation hardener	1.0
anisofac	Factor of anisotropic plastic response	1.0

797 Note: σ'_{v0} = initial vertical effective stress, and P_{atm} = atmospheric pressure (~100 kPa).

798 **Table 3**. Information of SPT boreholes at Ho Chi Minh City used in this study

District	Site	Location	Soil classification	Target *PGA* (g)
1	Vietcombank Tower 5 Me Linh Square, Ben Nghe Ward	10°46'32"N106°42'20"E	S_D	0.084770642
2	Sugarcane Project Ha Noi Boulevard, An Phu Ward	10°47'44"N106°45'22"E	S_D	0.085565749
3	Orchids Hotel 192 Pasteur, Ward 6	10°46'52"N106°41'45"E	S_D	0.084271152
4	Ben Van Don Apartment 278-283 Ben Van Don St., Ward 2	10°45'30"N106°41'40"E	S_D	0.084668705
5	Trieu Quang Phuc – Tran Hung Dao St. Intersection Ward 11	10°45'07"N106°39'41"E	S_D	0.077370031
6	231 Tran Van Kieu St., Ward 1	10°44'32"N106°37'40"E	S_D	0.069979613
7	Saigon Design Center Project C7-A01, Tan Phu Ward	10°43'34"N106°43'37"E	S_D	0.084566769
8	Ngo Han Office Buidling 172/39/39E An Duong Vuong St., Ward 16	10°43'36"N106°37'18"E	S_D	0.074475025
9	Office Building Phuoc Long B Ward	10°49'04"N106°46'47"E	S_D	0.074678899
10	Shopping Mall No. 106, 3/2 St., Ward 12	10°46'33"N106°40'48"E	S_D	0.077675841
11	Sacombank Office Building 920 Nguyen Chi Thanh St, Ward 4	10°45'24"N106°39'04"E	S_D	0.070071356
12	Hung Ngan Apartment 48A, Thi Muoi St., Tan Hung Thuan Ward	10°51'31"N106°37'50"E	S_D	0.081274210
Binh Chanh	Long An Metallurgical Office Building C12/15E QL1A, Tan Kien Commune	10°42'40"N106°35'58"E	S_D	0.058878695
Binh Tan	Tan Binh 2 industrial zone, Binh Hung Hoa Ward	10°49'13"N106°36'43"E	S_D	0.069979613
Binh Thanh	Viet Thuan Thanh Office Buidling 131 Dien Bien Phu St., Ward 15	10°47'48"N106°42'10"E	S_D	0.085270133
Cu Chi	WGH3+6Q2 Golf Resort Tan Thong Hoi Commune	10°55'42"N106°30'15"E	S_D	0.08077472
Go Vap	CTK Apartment Tan Son St., Ward 12	10°49'42"N106°38'32"E	S_D	0.083170234
Nha Be	Saigon International Hospital Project Tan An Huy residential area, Phuoc Kieng Commune	10°43'19"N106°42'23"E	S_D	0.081875637

Phu Nhuan	Hoang Minh Giam Apartment 8 Hoang Minh Giam, Ward 9	10°48’32”N106°40’24”E	S_D	0.084373089
Thu Duc	Song Da Riverside Apartment 623 QL13 St., Hiep Binh Phuoc Ward	10°51’17”N106°43’16”E	S_D	0.072670744
Tan Binh	Hoang Hoa Tham Apartment 171 A Hoang Hoa Tham St., Ward 13	10°48’20”N106°38’49”E	S_D	0.070173293
Tan Phu	Luy Ban Bich Wedding and Event 568 Luy Ban Bich St., Hoa Thanh Ward	10°47’09”N106°38’12”E	S_D	0.070173293
Hoc Mon	Nhi Xuan Industrial Zone Nguyen Van Bua St., Xuan Thoi Son Commune	10°52’22”N106°31’43”E	S_D	0.080173293
Can Gio	Can Gio Water Supplying Station Long Hoa Commune	10°27’20”N106°53’26”E	S_D	0.061783894

799

800 **Table 4**. Selected earthquake events from the NGA-West2 database

No.	Earthquake name	Year	Station	(M_w)	Mechanism	R_{rup} (km)	V_{s30} (m/s)
1	San Fernando	1971	Pasadena - Old Seismo Lab	6.61	Reverse	21.5	969.07
2	Whittier Narrows-01	1987	Pasadena - CIT Kresge Lab	5.99	Reverse Oblique	18.12	969.07
3	Loma Prieta	1989	Piedmont Jr High School Grounds	6.93	Reverse Oblique	73	895.36
4	Loma Prieta	1989	Point Bonita	6.93	Reverse Oblique	83.45	1315.92
5	Loma Prieta	1989	SF - Pacific Heights	6.93	Reverse Oblique	76.05	1249.86
6	Loma Prieta	1989	So. San Francisco_ Sierra Pt.	6.93	Reverse Oblique	63.15	1020.62
7	Northridge-01	1994	LA - Wonderland Ave	6.69	Reverse	20.29	1222.52
8	Northridge-01	1994	Vasquez Rocks Park	6.69	Reverse	23.64	996.43
9	Kobe_ Japan	1995	Kobe University	6.9	Strike-slip	0.92	1043
10	Chi-Chi_ Taiwan-05	1999	HWA002	6.2	Reverse	45.03	789.18
11	Chi-Chi_ Taiwan-05	1999	TTN042	6.2	Reverse	85.17	845.34
12	Umbria-03_ Italy	1984	Gubbio	5.6	Normal	15.72	922

801

802 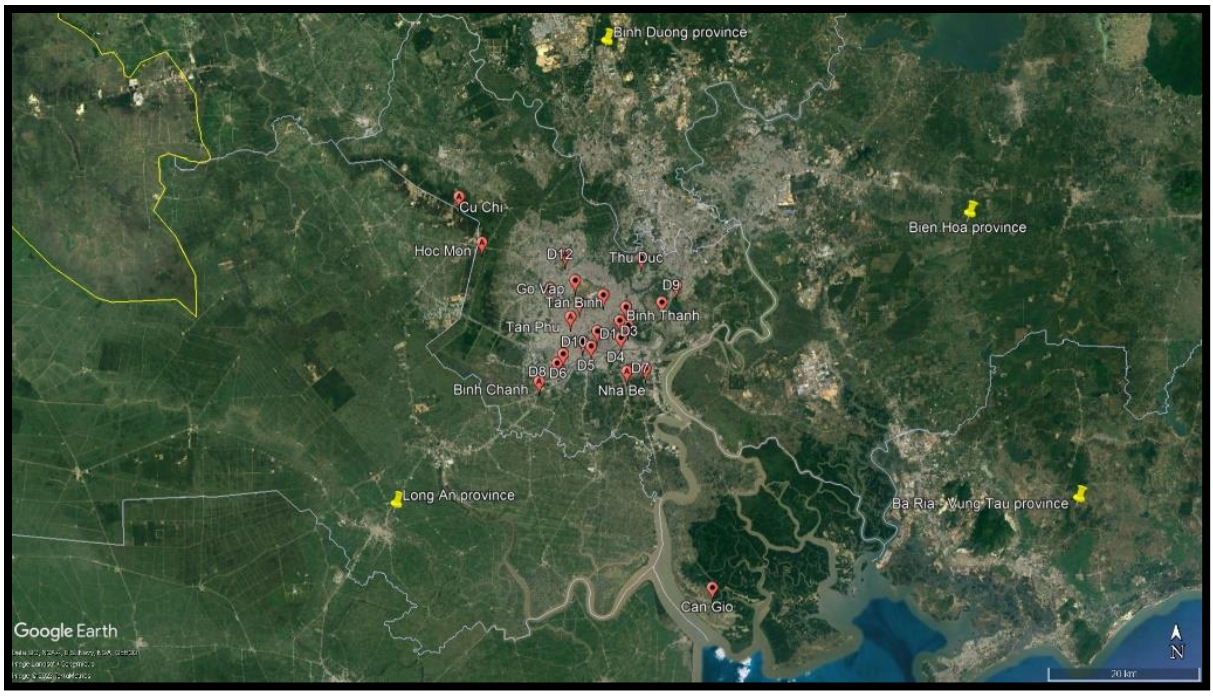

803 **Figure 1.** Locations of the observed boreholes in Ho Chi Minh city.

804

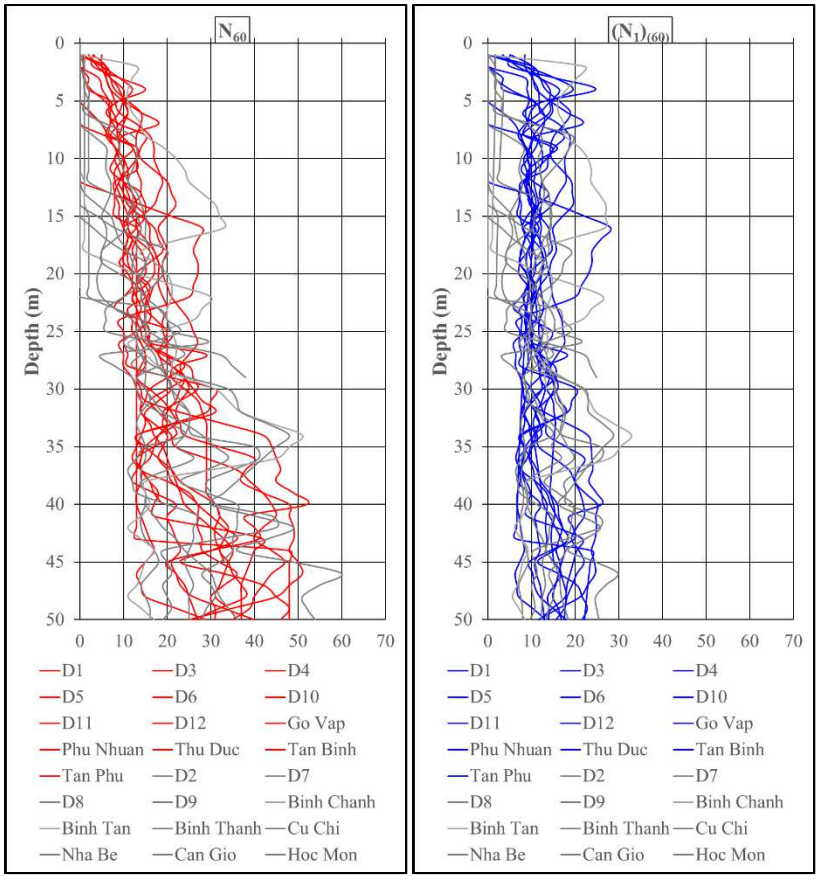

805

806 **Figure 2.** SPT number of blow counts (N_{60}) and corrected SPT number of blow counts $(N_1)_{60}$ of

807 boreholes used in this study. Noted: data with the grey solid line will not be considered in the

808 analysis.

809

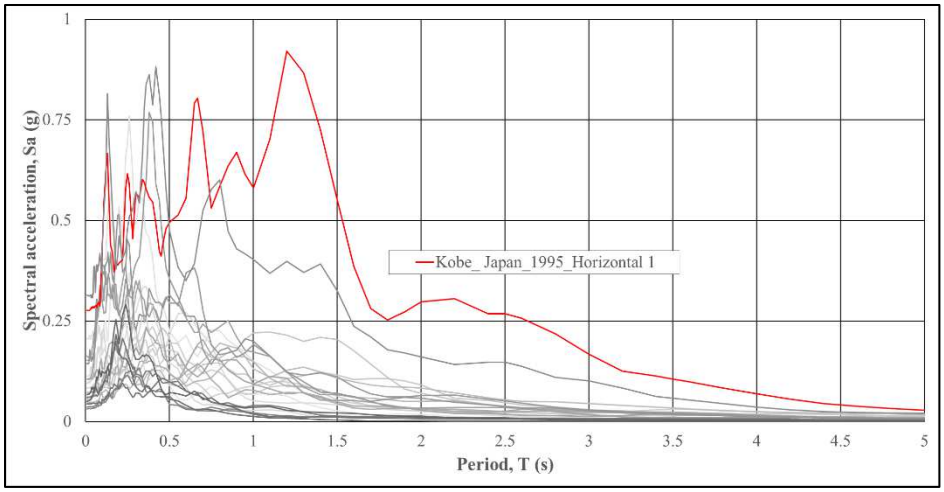

Figure 3. Response spectra of selected earthquake events from the NGA-West2 database.

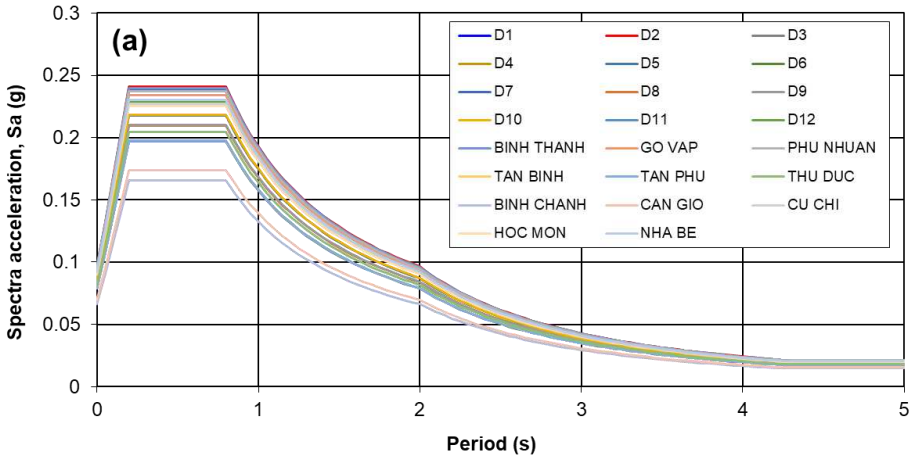

813

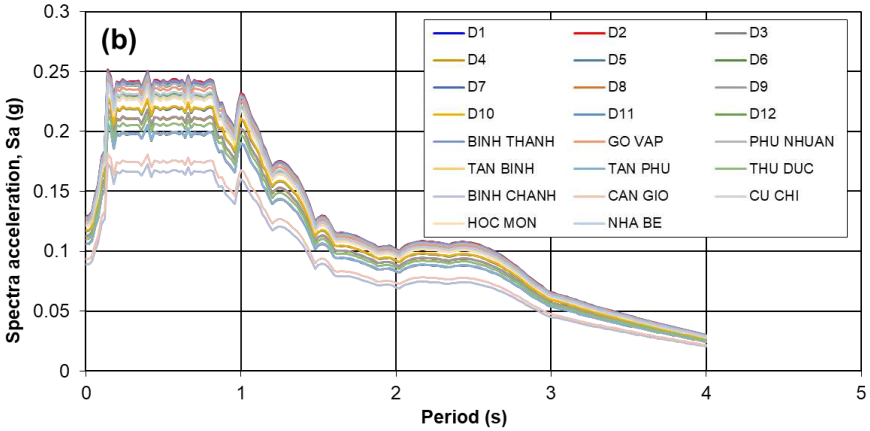

814

815 **Figure 4.** (a) Target response spectra and (b) matching response spectra to TCVN 9386:2012

816 with respect to Ho Chi Minh City locations.

817

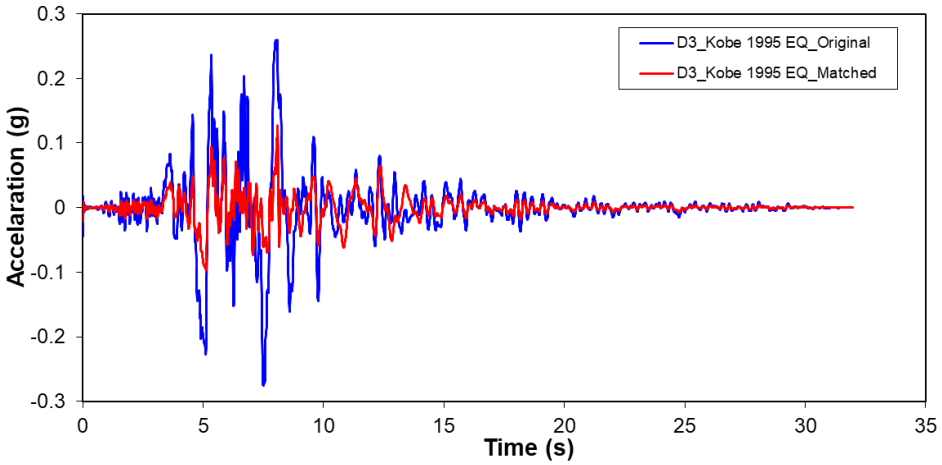

818

819 **Figure 5.** Acceleration time-history of the original 1995 Kobe earthquake and matched motion to

820 the target spectra at District 3, Ho Chi Minh City in accordance with TCVN 9386:2012.

821

822

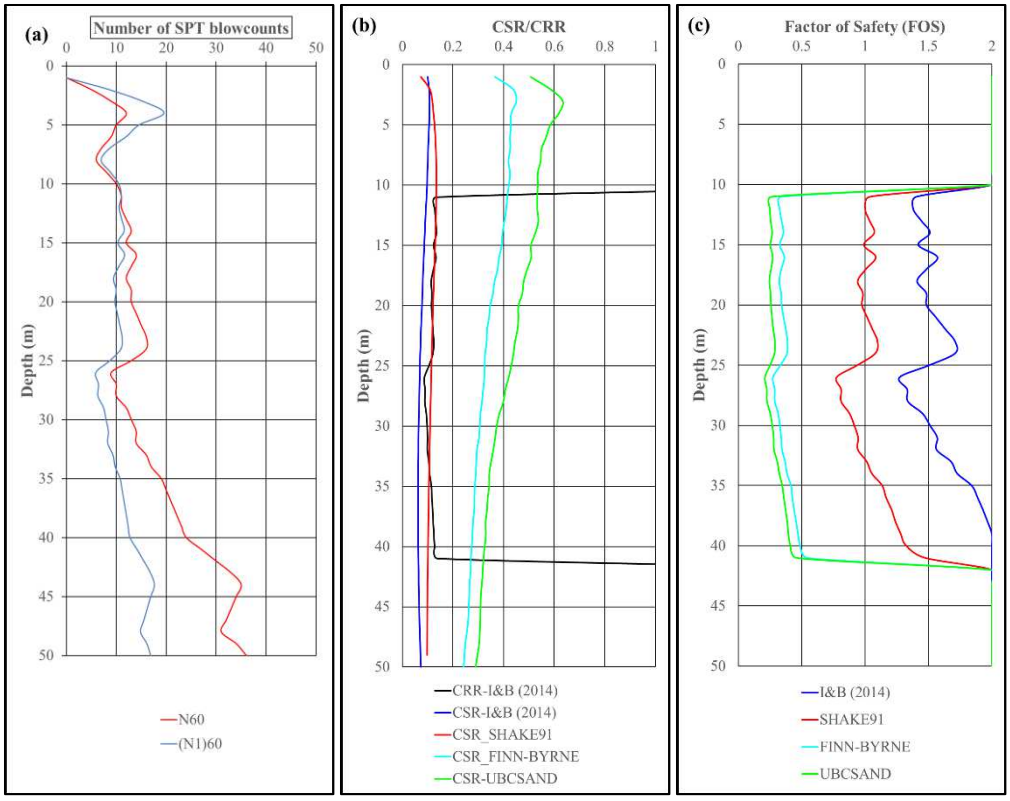
(a)
Number of SPT blowcounts
0 10 20 30 40 50
Depth (m)
N60
(N1)60
(b)
CSR/CRR
0 0.2 0.4 0.6 0.8 1
Depth (m)
CRR-I&B (2014)
CSR-I&B (2014)
CSR_SHAKE91
CSR_FINN-BYRNE
CSR-UBCSAND
(c)
Factor of Safety (FOS)
0 0.5 1 1.5 2
Depth (m)
I&B (2014)
SHAKE91
FINN-BYRNE
UBCSAND

823

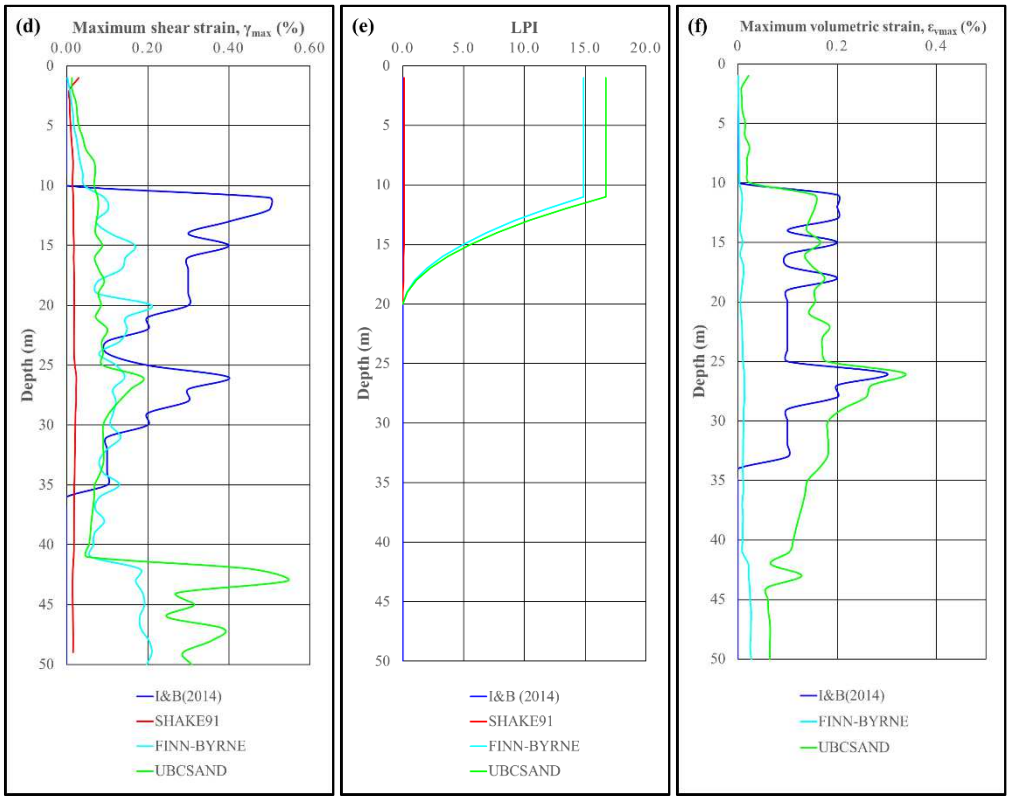
(d)
Maximum shear strain, γmax (%)
0.00 0.20 0.40 0.60
Depth (m)
I&B(2014)
SHAKE91
FINN-BYRNE
UBCSAND
(e)
LPI
0.0 5.0 10.0 15.0 20.0
Depth (m)
I&B (2014)
SHAKE91
FINN-BYRNE
UBCSAND
(f)
Maximum volumetric strain, εvmax (%)
0 0.2 0.4
Depth (m)
I&B(2014)
FINN-BYRNE
UBCSAND

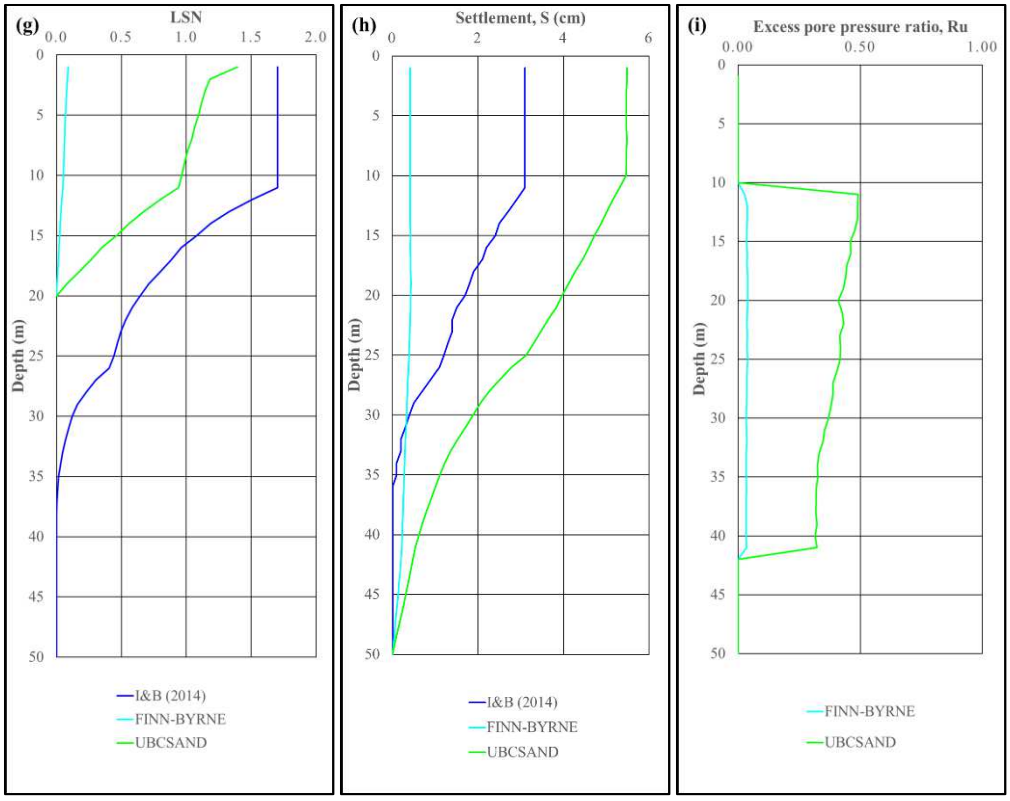

824

825 **Figure 6.** Comparison of alternative analyses of liquefaction evaluation for a SPT soil profile at

826 District 3 – Ho Chi Minh City in terms of (a) N_{60} and $(N_1)_{60}$, (b) *CSR/CRR*, (c) factor of safety

827 (*FS*), (d) maximum shear strain γ_{max}, (e) *LPI*, (f) maximum volumetric strain ε_v, (g) *LSN*, (h)

828 ground surface settlement (*S*), and (i) excess pore water pressure ratio (R_u) versus depth.

829

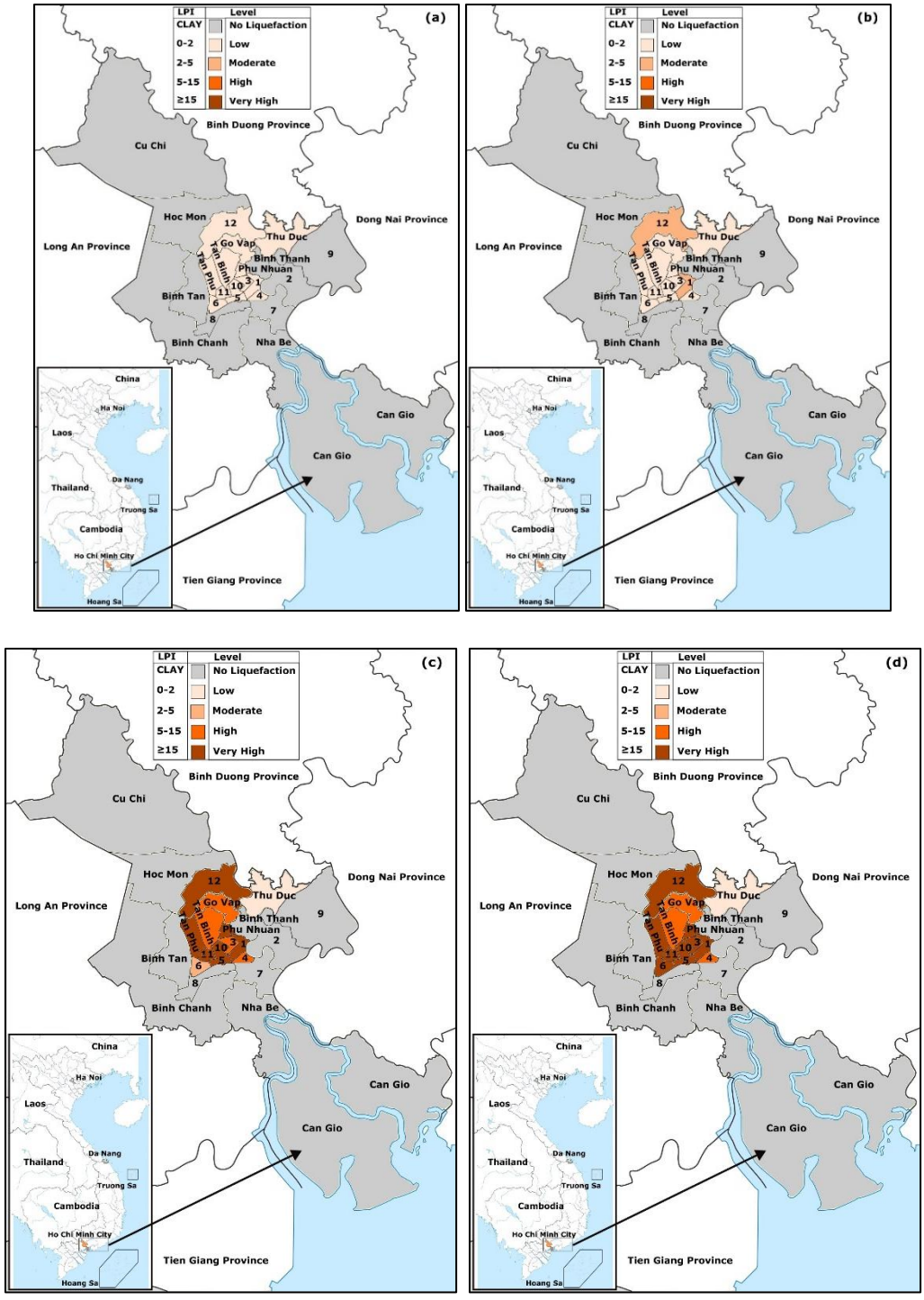

830

831 **Figure 7.** Distribution of liquefaction potential index (*LPI*) interpolated across the land of Ho

832 Chi Minh metropolitan city using alternative methods: (a) simplified method (Boulanger and

833 Idriss, 2014), (b) equivalent linear analysis (SHAKE91), (c) loosely-coupled effective stress

834 analysis (Finn-Byrne model), and (d) fully-coupled effective stress analysis (UBCSAND model)
835 based on available SPT database and target response spectra to TCVN 9386:2012.
836

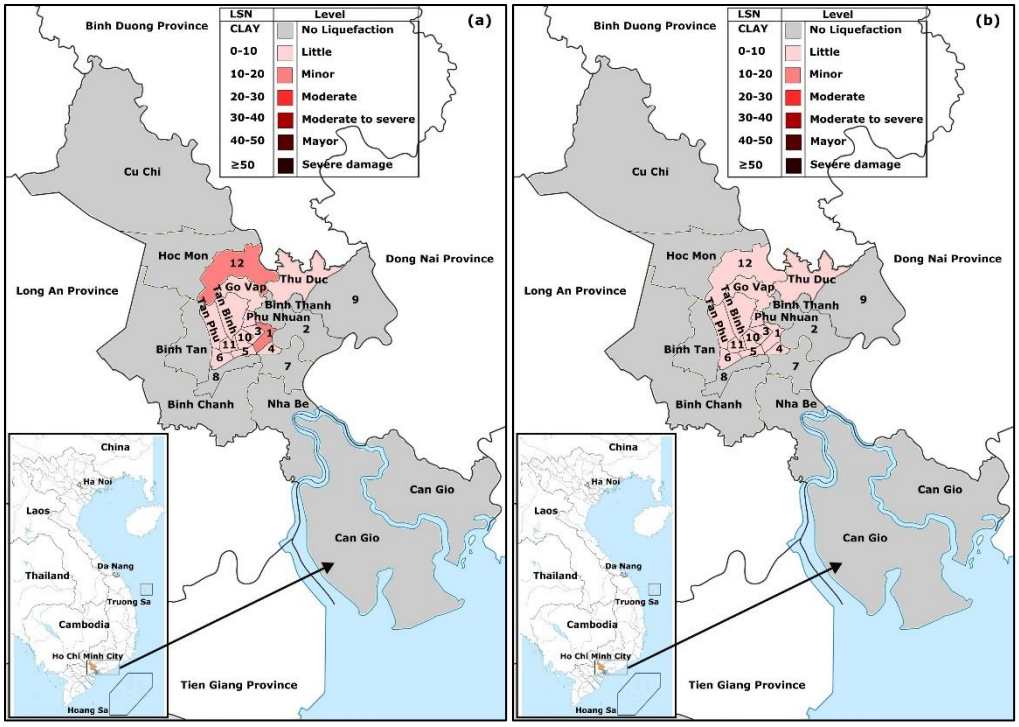

837

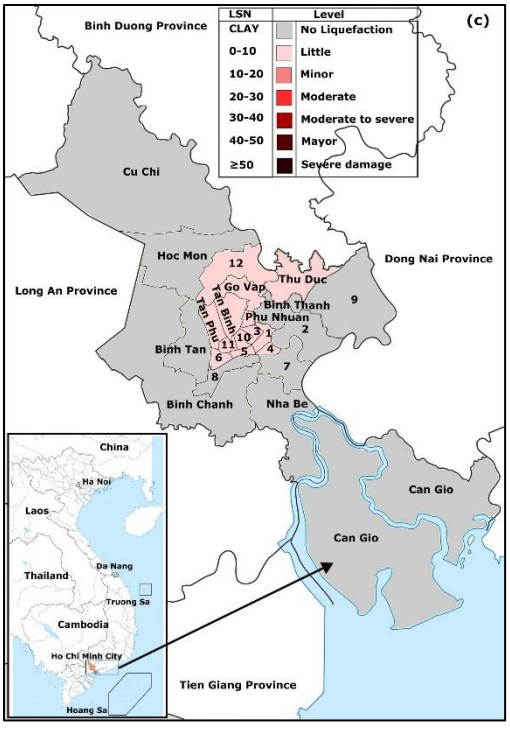

838

839 **Figure 8.** Distribution of liquefaction severity number (*LSN*) interpolated across the land of Ho

840 Chi Minh metropolitan city using alternative methods: (a) simplified method (Boulanger and

841 Idriss, 2014), (b) loosely-coupled effective stress analysis (Finn-Byrne model), and (c) fully-

842 coupled effective stress analysis (UBCSAND model) based on available SPT database and target
843 response spectra to TCVN 9386:2012.
844

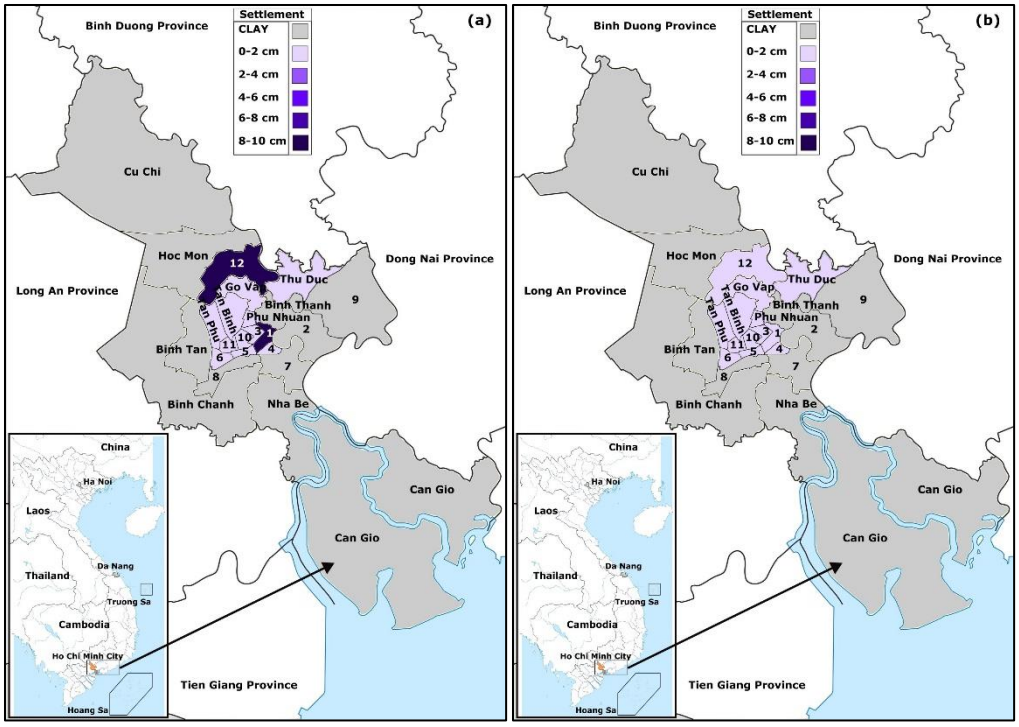

845

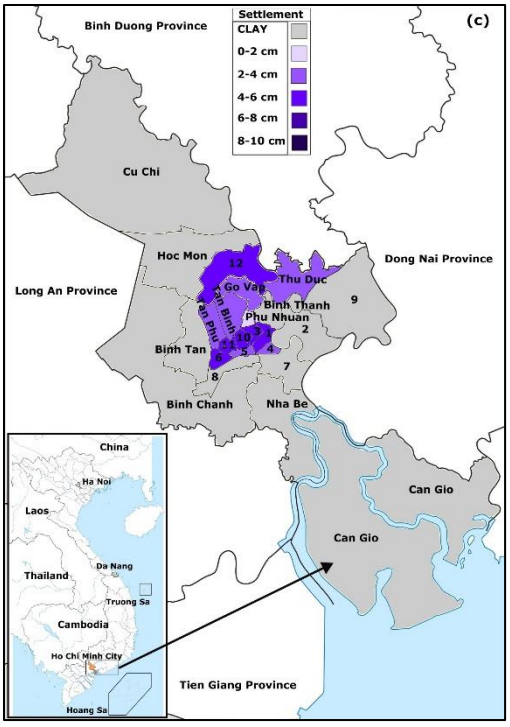

846

847 **Figure 9.** Distribution of surface ground settlement (*S*) interpolated across the land of Ho Chi

848 Minh metropolitan city using alternative methods: (a) simplified method (Boulanger and Idriss,

849 2014), (b) loosely-coupled effective stress analysis (Finn-Byrne model), and (c) fully-coupled

effective stress analysis (UBCSAND model) based on available SPT database and target response spectra to TCVN 9386:2012.